Interaction of the Pore-Forming Domain of Colicin A with Phospholipid Vesicles

Dominique Massotte, Jean-Louis Dasseux,[‡] Paul Sauve,[§] Marek Cyrklaff, Kevin Leonard, and Franc Pattus*

European Molecular Biology Laboratory, Meyerhofstrasse 1, Postfach 10.2209, 6900 Heidelberg, FRG

Received January 31, 1989; Revised Manuscript Received May 31, 1989

ABSTRACT: The interaction of the 20-kDa pore-forming domain of colicin A with phospholipid vesicles was investigated by gel permeation chromatography, analytical centrifugation, and electron microscopy. Under the experimental conditions of this study, this peptide was found to interact only with vesicles containing negatively charged phospholipids. It forms a well-defined disklike complex with phosphatidylglycerols with a preference for those containing 12–14 atoms of carbon in their fatty acid chain. This complex has a diameter of 120 Å and is about one bilayer thick. It contains nine molecules of peptide and is formed both at acidic pH (pH 5.0) and at neutral pH (pH 7.2).

Colicins are bactericidal proteins which kill sensitive *Escherichia coli* cells. Colicin A belongs to the group of colicins which collapse the membrane potential, presumably by forming ionic channels [Tokuda & Konisky, 1979; for a review, see Lazdunski et al. (1988)]. These colicins, although water-soluble, can form voltage-gated ionic channels in artificial membranes (Shein et al., 1978; Collarini et al., 1987). They provide a very interesting model system for studying protein insertion into membranes and for studying channel voltage-gating. The C-terminal domain of colicin A, isolated after thermolysin digestion, carries the pore-forming activity (Martinez et al., 1983). It has been crystallized (Tucker et al., 1986) and the structure of the water-soluble form recently solved (Parker et al., 1989). A tentative model of the mechanism of membrane insertion of the pore-forming domain of colicin A, based on this soluble structure, has been proposed. This model implies, first, electrostatic interaction with negatively charged lipids in the membrane and then insertion of the hydrophobic helical hairpin initially buried in the soluble structure (Parker et al., 1989). Although previous studies have shown that colicin A interacts preferentially with negatively charged phospholipids (Pattus et al., 1983), quantitative data on the influence of the polar headgroup and acyl chain length of the interaction of the C-terminal domain of colicin A with phospholipid membranes are still lacking. There is, also, little direct information regarding the secondary, tertiary, and quaternary structures of the membrane-bound forms of colicin A and its C-terminal peptide.

In the present study, we have investigated, by gel filtration, electron microscopy, and analytical centrifugation, the interaction of the pore-forming domain of colicin A with lipid vesicles of defined composition. We have found that this domain binds exclusively to negatively charged phospholipid vesicles and forms a well-defined complex with various phosphatidylglycerols, especially those having only 12–14 carbon atoms in their fatty acid chains.

Materials and Methods

Dimyristoylphosphatidylglycerol (DMPG) and dilauroylphosphatidylglycerol (DLPG) were purchased from Avanti Polar Lipids Inc., dipalmitoylphosphatidylglycerol (DPPG), dioleoylphosphatidylglycerol (DOPG), and dimyristoylphosphatidylcholine (DMPC) were obtained from Sigma, and [^{14}C]dipalmitoylphosphatidylethanolamine (DPPE) was from New England Nuclear. They were used without further purification. DLPG and DMPG gave a single spot by thin-layer chromatography and underwent a phase transition at the expected transition temperature (T_c) as judged by fluorescence polarization of diphenylhexatriene embeded in unsonicated dispersions of the lipids (Dasseux et al., 1984).

Cell Growth and Protein Purification. Colicin A was purified from *Citrobacter freundii* strain CA31 and was converted into its thermolytic fragment as described previously (Cavard & Lazdunski, 1979; Tucker et al., 1986). The C-terminal peptide was purified by filtration on a Sephadex G50 column, dialyzed against water, and lyophilized. The lyophilized peptide was dissolved in the desired buffer, and the solution was spun in an airfuge to remove suspended particles before use. Protein concentrations were measured with the interference optics of the Model E ultracentrifuge according to Babul and Stellwagen (1969), by using a capillary-type synthetic boundary centerpiece. Equation 1 was used for

$$J_r = (dn/dc)ec/\lambda \quad (1)$$

calculation, where J_r is the number of displaced fringes, dn/dc the specific refractive increment, e the thickness of the double-sector centerpiece, c the solute concentration, and λ the wavelength of monochromatic light. The molar extinction coefficient (E_{280} = 2.43 × 10^{-4} M^{-1} cm^{-1}) at 280 nm of the thermolytic fragment found by this method is higher than the theoretical coefficient based on the content of aromatic amino acids (E_{280} = 2.03 × 10^{-4} M^{-1} cm^{-1}).

Preparation of Lipid Vesicles. Twenty milligrams of phospholipid was labeled with 0.1% (w/w) [^{14}C]DPPE by mixing in methanol/benzene (1:6 v/v) followed by lyophilization. Sonication was performed with a sonication probe (B12 sonifier, Bransonic Co.) in 1 mL of Hepes (50 mM)/NaN_3 (3 mM) adjusted to pH 7.2 with NaOH (buffer A) or in 1 mL of Tris (50 mM)/EDTA (7.5 mM)/EGTA (7.5 mM)/NaN_3 (3 mM) adjusted to pH 5.0 with acetic acid (buffer B). The vesicle suspension was then centrifuged in a bench centrifuge for 5 min.

Gel Filtration Chromatography. Gel filtration experiments were carried out at 37 °C with a Sepharose CL 6B column (1.6 × 83 cm) equilibrated in buffer A (pH 7.2) or B (pH 5). In order to prevent aspecific adsorption of protein and lipids

* To whom correspondence should be addressed.

‡ Present address: Holphar Arzeimittel GmbH, Justus-von-Liebig-Strasse 16, D-6603 Sulzbach, FRG. Recipient of a European Molecular Biology Organization fellowship.

§ Present address: Centre de Biochimie et Biologie Moléculaire, CNRS, 31 Chemin Joseph Aiguier, F-13009 Marseille, France.

0006-2960/89/0428-7713$01.50/0

on the gel matrix, peptide and lipid mixtures were passed twice through the column. The recovery yields were then higher than 70–80%. Phospholipids and thermolytic fragment were mixed together at the desired mole/mole ratio (R_i) in a final volume of 300 μL and incubated for 10 min at 37 °C (except for DPPG, 42 °C). The sample was then loaded on the column. Fractions of 1 mL were collected, and lipid content was estimated by counting radioactivity. Protein concentration was determined by the Bio-Rad assay.

Column calibration with proteins of known Stokes radii was done according to le Maire et al. (1987) using the partition coefficient, K_D, defined as

$$K_D = (V_e - V_0)/(V_t - V_0)$$

where V_e is the elution volume of the protein, V_0 is the void volume, and V_t is the total volume of the column.

Electron Microscopy. Negatively stained specimens were prepared by using the Valentine technique (Valentine et al., 1968). Thin carbon films were prepared by evaporation onto freshly cleaved mica. The films were floated off the mica onto a small volume of sample for 10 s and then onto a solution of stain (1% aqueous uranyl acetate, pH 5.5) for 10 s and then picked up on a copper 600-mesh grid and blotted dry. Images were made in a Philips EM 400T electron microscope operating at 80 kV and 36000x magnification. Vitrified lipid–protein complexes were prepared as described by Adrian et al. (1968). A drop of suspension was deposited on a perforated carbon film treated by glow discharge in air. While keeping a humid environment to prevent water evaporation, the grid was mounted on a guillotine-like frame. Excess liquid was removed with filter paper and the guillotine released immediately, plunging the grid into a cryostat of liquid ethane. The electron microscope (Philips EM400 operated at 80 kV) was fitted with an improved blade-type anticontamination device (Homo et al., 1984). Frozen specimens were inserted into the cryo-specimen holder (Gatan Model 626) under liquid nitrogen and rapidly inserted into the electron microscope.

Analytical Centrifugation. In all experiments, glass-distilled water was used. Standard buffer solutions contained 50 mM Tris–acetate/15 mM EDTA at pH (or pH#)[1] 5.0. The partial specific volume of the protein, $\bar{V}_p = 0.718 \pm 0.0004$ cm^3/g, was measured in an Anton Paar Model DMA 02c precision densimeter. The partial specific volume was in good agreement with the partial specific volume, $\bar{V}_p = 0.707$ cm^3/g, calculated from the amino acid composition using the amino acid partial specific volumes determined by Bull and Breese (1974) but was somewhat lower than with the commonly used data from Cohn and Edsall (1943), $\bar{V}_p = 0.747$ cm^3/g. The partial specific volume of DMPG measured in the Anton Paar densimeter at 25 °C was $\bar{V}_l = 0.914$ cm^3/g.

The ultracentrifugation studies were performed with a Beckman-Spinco AE analytical centrifuge equipped with an RITC temperature control unit and an electronic speed control system. Prior to the experiments, the samples were dialyzed to equilibrium against standard buffer. Sedimentation velocity experiments were conducted at 25 °C, at 58 083 rpm, in aluminum-filled Epon double-sector cells having 12-mm centerpieces with sapphire windows. The schlieren optical system was used. Samples (400-μL solutions of protein, lipid, or lipid–protein complex) were placed in one side of the 12-mm double-sector cell, and dialysis buffer was in the other sector. After a constant rotor speed was reached, pictures of schlieren patterns were taken at 4-min intervals (10 pictures), and the images were traced at 10× magnification using a Priox projector. The apparent sedimentation coefficients determined in their respective solutions (s_{25}) were calculated from

$$\mathrm{d} \ln x/\mathrm{d}t = s_{25}\omega^2 \quad (2)$$

where x is the distance of the sedimentation boundary from the axis of rotation and ω is the angular velocity in radians per second. These s_{25} values were then corrected for the viscosity and the density of buffer relative to water to give $s_{25,w}$. The protein concentration used was 5 mg/mL and the lipid concentration adjusted to obtain the desired protein/lipid molar ratio (R_i). Meniscus depletion, sedimentation equilibrium experiments (Yphantis, 1964) were carried out in a 12-mm double-sector cell with an aluminum-filled epon centerpiece using interference optics. Samples (100-μL solutions of the lipid–protein complex) were equilibrated for at least 48 h against buffer at 25 °C and placed in one sector, and the dialysis buffer was in the other sector. Protein concentration was 1.5 mg/mL. The equilibrium studies were carried out at 14 000–250 000 rpm for the protein–lipid complex and at 42 000 rpm for the thermolytic fragment alone at 25 °C. Images were recorded after 24 and 30 h. The interference patterns on the photographic plates were magnified, and the vertical fringe deplacement ($Y - Y_0$) was measured with a Nikon Model 6C T2 profile projector. The conversion factor used for fringes to thermolytic fragment concentration was 4.0 fringes L^{-1} g^{-1} (Babul & Stellwagen, 1969).

The apparent molecular weight (M^*) was calculated according to

$$\frac{\mathrm{d} \ln (Y - Y_0)}{\mathrm{d}r^2} = \frac{M^*(1 - \phi'\rho)\omega^2}{RT} \quad (3)$$

where ϕ' is the partial specific volume, ρ is the density of the solvent, R is the gas constant, and ω is the angular rotor velocity. In the case of the lipid–protein complexes, where M^* is the mean molecular weight of the entire complex [$M^* = M(1 + \delta_l)$], M is the protein molecular weight and δ_l the fraction of bound lipids (W_l/W_p). ϕ', the corresponding partial specific volume, was calculated according to Tanford et al. (1974):

$$\phi' = (\bar{V}_p + \delta_l\bar{V}_l)/(1 + \delta_l) \quad (4)$$

where $\bar{V}_p$ and $\bar{V}_l$ are the partial specific volumes of protein and lipid, respectively. δ_l was determined as described below.

Determination of the Molecular Weight of the Protein Moiety in Protein–Lipid Complexes. The sedimentation equilibrium experiments for complex formation between the thermolytic fragment and DMPG were done by the method of Reynolds and Tanford (1976). With this method, it is possible to determine the molecular weight of the protein moiety in a lipid–protein complex by masking the lipid part at a solvent density $\rho = 1/\bar{V}_l$ ($\bar{V}_l$ is the partial specific volume of the lipid), using different $^2H_2O/H_2O$ mixtures. In eq 5, derived by Casassa and Eisenberg (1964):

$$M(1 - \phi'\rho) = M[(1 - \bar{V}_p\rho) + \delta_l(1 - \bar{V}_l\rho)] \quad (5)$$

where M is the molecular weight of the protein (excluding bound lipid), ϕ' is the apparent partial specific volume of the protein bound to lipid, $\bar{V}_p$ is the true specific volume of the protein, and δ_l is the binding ratio (W_l/W_p). The second term in the right-hand vanishes at this density, and ϕ' equals $\bar{V}_p$.

Results

Evidence for the Formation of a Well-Defined Complex with DMPG. Incubation of the thermolytic fragment of colicin

[1] pH#: uncorrected pH meter reading in $^2H_2O/H_2O$ mixtures.

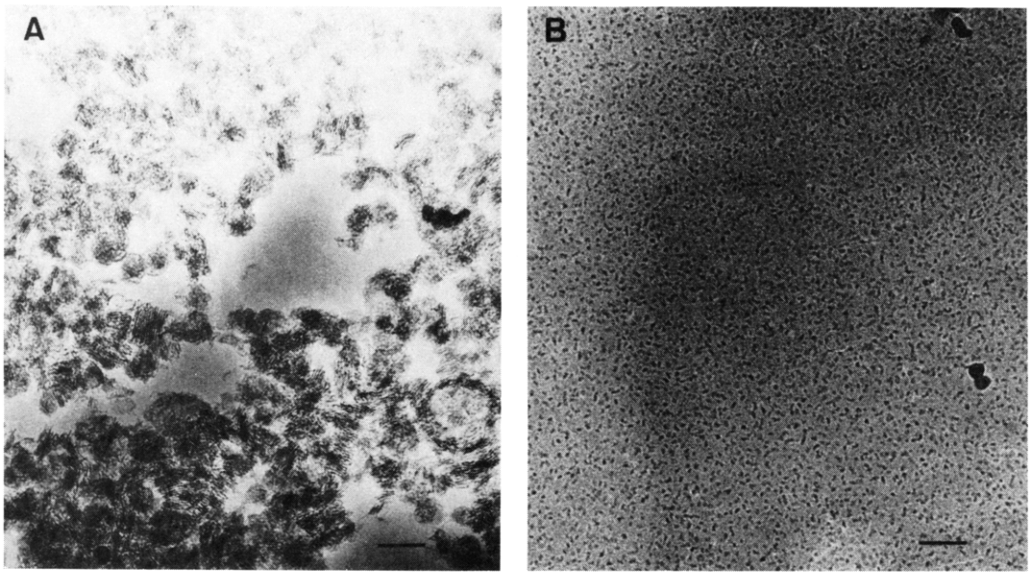

FIGURE 1: Images of DMPG vesicles incubated with the C-terminal thermolytic fragment of colicin A (lipid/protein molar ratio R_i = 25). Samples are embedded in vitrified ice. (A) The incubation was carried out at 4 °C well below the lipid phase transition temperature (23 °C). (B) Same as (A), but the temperature was raised to 37 °C before embedding in ice. The bar in both figure represents 200 nm. Buffer B, pH 5.0.

A with DMPG vesicles at pH 5.0 below the phase transition of DMPG (T_c = 20 °C) produces a dramatic increase in the turbidity and formation of a heavy precipitate. Upon raising the temperature above T_c, the suspension undergoes complete clarification, indicating complete reorganization of the lipid structure. Cooling down the mixture below T_c again did not cause further precipitation. The cryoelectron micrographs shown in Figure 1A,B were taken from samples maintained before vitrification below and above the phase transition temperature, respectively. The aggregates at low temperature consist of stacked membranes with a repeating unit of 92 ± 17 Å (Figure 1A). Above T_c, only dispersed small particles (60-Å diameter) are seen (Figure 1B). Note that no lipid bilayer structures are visible.

In order to characterize the nature of the particle observed under the microscope, the thermolytic fragment mixed together with DMPG vesicles at various lipids/protein molar ratios was incubated and eluted on Sepharose CL 6B at 37 °C. The experiments were performed both in neutral (pH 7.2) and in acidic (pH 5) conditions. DMPG vesicles elute as a homogeneous peak at a position close to the void volume of the column (Figure 2A). The thermolytic fragment elutes as a single symmetrical peak at the elution volume of aldolase from rabbit muscle, a protein with a radius of gyration (R_s) of 4.6 nm. This abnormal elution volume does not mean that, in solution, the peptide is an oligomer but reflects either the elongated shape of the peptide or an unusual permeation behavior. Analytical centrifugation analysis clearly shows that the thermolytic fragment is monomeric in solution in a wide range of pH values and concentrations (see below) as shown with colicin A previously (Cavard et al., 1988).

The elution diagram of various DMPG/protein mixtures at pH 7.2 is shown in Figure 2B–E. At an R_i = 33, the protein elutes as a single symmetrical lipoprotein peak. This lipid–protein complex is characterized by an R_s of about 55 Å and an equivalent molecular weight of 280 000, as estimated from the column calibration (Table I). At lower R_i's, the elution diagram from Figure 2 shows two peaks: one corresponds to free peptide while the other elutes at a similar position to the complex at R_i = 33. Above the molar ratio of 33, the complex is enriched in lipids as seen from its size increase (Table I). Vesicles containing proteins appear at ratios as high as 130

Table I: Size of the Complex Formed by the Colicin A Thermolytic Fragment and Phosphatidylglycerol of Various Chain Lengths at pH 7.2

lipid	$C_{X:Y}$	R_i	R_s[a] (Å)	no. of peaks[b]
DLPG	12:0	≤33	51	2
		>33	54	1
DMPG	14:0	4	51	2
		8	53	2
		16	53	2
		33	55	1
		50	57	1
		65	58	1
DPPG	16:0	≤33	58	2
		>33	69	3
DOPG	18:1	≤33	61	3

[a] R_s, radius of gyration estimated from column calibration. [b] Number of peaks eluted from the Sepharose CL 6B column.

(Figure 2E). Previous experiments with colicin A and the thermolytic fragment with lipid monolayers (Pattus et al., 1983; Frenette et al., 1989) have shown that the affinity of the proteins increases drastically at acidic pH. We therefore compared the elution profile of DMPG/peptide mixtures at pH 7.2 and 5.0. Surprisingly, almost identical results were obtained at pH 5.0. The elution profiles obtained at pH 5.0 were surimposable onto those obtained at pH 7.2 shown in Figure 2. A single complex elutes at R_i = 25 with an R_s = 55 Å. This complex partially dissociates at lower R_i values. The only difference found is that at pH 5.0 at R_i = 3, the thermolytic fragment precipitates heavily. Increasing the molar ratio up to R_i = 9 redissolves the precipitate, indicating some reversibility in the process.

To learn more about the size and the composition of the complex formed by the C-terminal domain of colicin A with DMPG and to confirm the gel permeation liquid chromatography results by an independent method, we investigated the sedimentation velocity behavior of colicin A thermolytic fragment/DMPG mixtures at pH 5.0 and the equilibrium sedimentation of the complex at R_i = 26 at different solvent densities in an analytical ultracentrifuge. Typical sedimentation patterns of the thermolytic fragment at a DMPG/protein ratio ranging from R_i = 0 to R_i = 50 (pH 5.0) are shown in Figure 3. At R_i = 26, one sharp and symmetrical peak was obtained after 16 and 24 min at 58 000 rpm, indi-

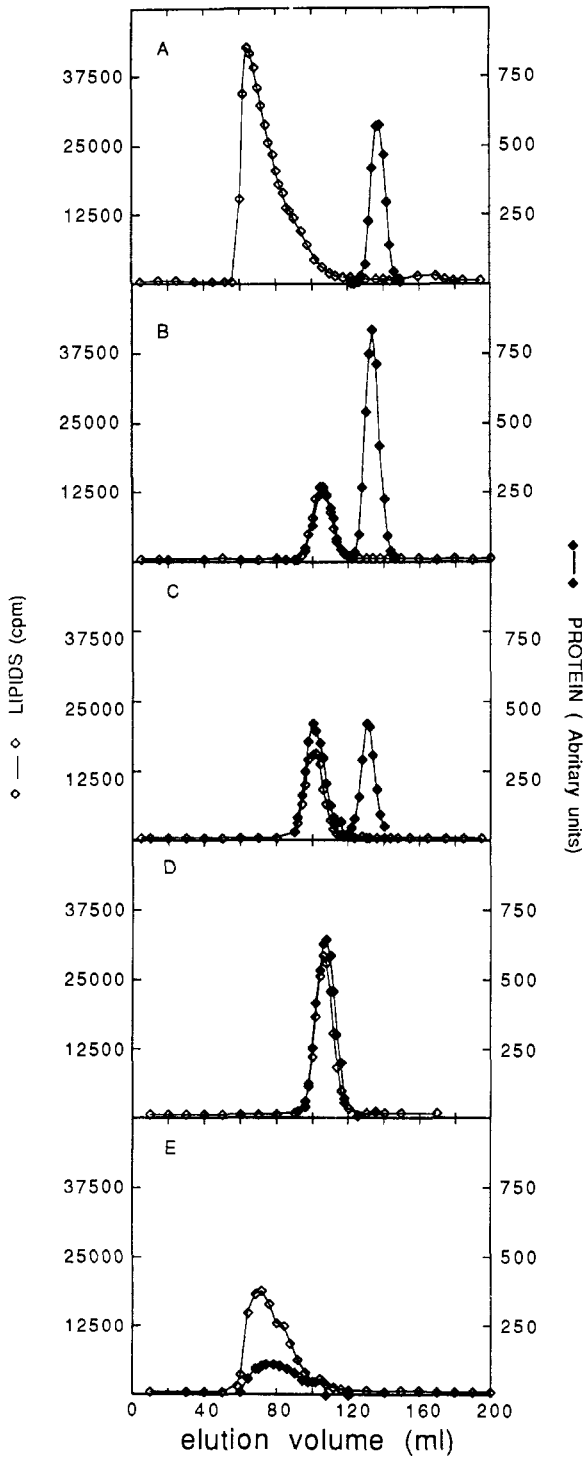

FIGURE 2: Sepharose CL 6B elution profiles of DMPG unilamellar vesicles incubated with colicin A pore-forming fragment. (A) Lipid vesicles or peptide alone. (B–E) correspond to R_i = 8, 17, 33, and 130, respectively. (◇) ^{14}C radioactivity of lipids; (◆) protein concentration. Buffer A, pH 7.2.

cating a substantial homogeneous complex with a sedimentation coefficient $s_{25,w}$ = 8.6 S. At R_i = 12, two peaks are clearly resolved: one corresponding to the front of free peptide monomers ($s_{25,w}$ = 2.3 S) and one to the front of the lipid–protein complex ($s_{25,w}$ = 10.0 S). There is a complete correlation between the analytical centrifugation data and those obtained from gel filtration experiments. Both methods show that for $R_i \leq 26$, there is an equilibrium between monomeric peptide and a complex with an $s_{25,w}$ = 8.4 and R_s = 55 Å. Increasing R_i above 26 results in an increase in both the $s_{25,w}$ and R_s of the complex ($s_{25,w}$ = 13.8 S and R_s = 57 Å for R_i = 50 at pH 5.0; see also Table I).

Equilibrium sedimentation experiments were conducted for R_i = 0 and for R_i = 26, 1, and 1.5 mg/mL protein concentration, at 42 500 and 14 000 rpm, respectively. For both R_i values, the plot of the logarithm of the protein concentration versus the square of the distance from the center of rotation (r^2) was linear, indicating homogeneity of the sedimented particle. The apparent molecular weight calculated from eq 3 was 18 900 ± 300 for R_i = 0 and 320 300 ± 4500 for the whole complex at R_i = 26. The value for the free peptide in solution (18 900), which is consistent with the molecular weight calculated from its amino acid sequence (21 790), shows that the thermolytic fragment is monomeric at this concentration. As discussed above, the much higher molecular weight found by gel filtration is probably due to nonideal behavior in the column.

Determination of the Composition of the Lipid–Protein Complex by Sedimentation Equilibrium Studies. The sedimentation equilibrium measurements, to determine the composition of the complex formed by the C-terminal peptide of colicin A and DMPG, were done at 25 °C at different solvent densities by varying the $^2H_2O/H_2O$ ratio (Reynolds & Tanford, 1976). At each density, at the slowest possible speed, the overall ln c vs r^2 plot, where c is the protein concentration at the radial position r, showed no significant upward curvature, and therefore the value for $M(1 - \phi'\rho)$ was calculated by using the least squares of the entire plot. All measurements were done at R_i = 26 where no more free thermolytic fragment could be detected by gel filtration chromatography and where the complex sediments as one homogeneous entity (see above). The apparent molecular weights for the protein part of the complex as a function of the density are shown in Figure 4. The graph is linear with a correlation coefficient r = 0.995. The solid lines indicate the point where $\rho = 1/\bar{V}_l$, that is, the point where lipids do not contribute to the molecular weight of the particle. The corresponding molecular weight for the protein part of the complex is 201 000 ± 7000. From the molecular weight of the colicin A thermolytic fragment being 21 790, it can be concluded that there are nine molecules in the complex (N = 9.2 ± 0.3). From the slope which is equal to $d[M(1 - \phi'\rho)]d\rho = -M(\bar{V}_p + \delta_l\bar{V}_l)$, the binding ratio δ_l or the mass of bound lipids $M\delta_l$ and thus the number of lipid monomers in the complex can be obtained. This yields a number of bound lipids of 203 ± 28 in the complex. This corresponds to a true lipid/protein molar ratio of 22 ± 4, which is, within experimental error, similar to the R_i of the sample used. This indicates that most of the colicin A thermolytic fragment is in its lipid-bound form at this lipid/protein ratio.

To get a better idea of its size and shape, we looked at this complex under the electron microscope. Because of lack of contrast, cryoelectron microscopy of unstained specimens did not produce well-defined pictures of the complex (see Figure 1B). However, by negative staining using the Valentine method, the size and the shape of the complex could be clearly resolved. The lipid-protein complex as seen by negative staining is shown in Figure 4. In accordance with gel filtration and analytical centrifugation, the size distribution of the particles at R_i = 25 is quite narrow. The complex is a disklike particle 60 Å thick and 120 Å in diameter, which is also in good agreement with the R_s of 55 Å found by gel filtration. No substructures can be resolved on these images apart from the darker center of the disk. This darker center may be a hole or positive staining of lipid.

Influence of the Fatty Acid Chain Length and the Nature of the Phospholipid Headgroup. Phosphatidylglycerols with

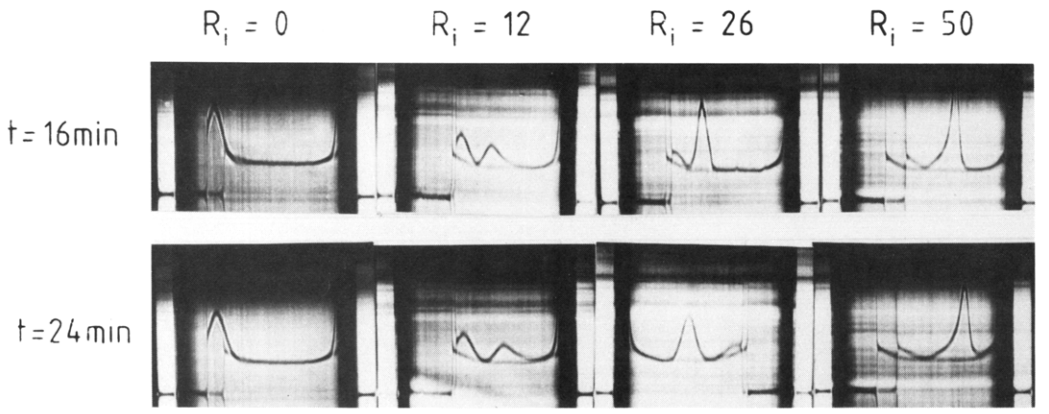

FIGURE 3: Sedimentation patterns yielded by DMPG/colicin A C-terminal peptide mixtures (buffer B, pH 5.0). Only pictures taken after 16 and 24 min at 58 083 rpm are reproduced, but the peaks remained symmetrical for longer time periods. The schlieren optical system was used.

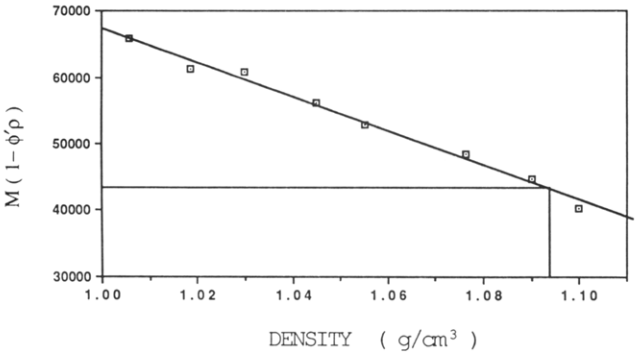

FIGURE 4: Plot of $M(1 - \phi'\rho)$ for the complex formed between the colicin A C-terminal 20-kDa fragment and dimyristoylphosphatidylglycerol (R_i = 26) versus solvent density (ρ) at 25 °C. M is the molecular weight of the protein part of the complex. All solutions were standard buffer, 1.5 mg/mL protein, and varying $^2H_2O/H_2O$ percentages. The lines correspond to the density of solvent matching the density of lipids.

saturated fatty acyl chains between 12 (DLPG) and 16 (DPPG) carbon atoms long, together with an 18-carbon singly unsaturated version (DOPG), were used to determine the influence of chain length on lipid–protein complex formation at 37 °C.

Quite similar gel filtration profiles to those shown with DMPG in Figure 2 were obtained with the shorter chain DLPG. At pH 7.2 and $R_i \leq 33$, a lipid complex with an R_s of approximately 51 Å is in equilibrium with peptide monomers. The size of this complex increases as R_i increases above 33 (Table I). At acidic pH in DLPG (pH 5.0), the elution profiles are similar to those observed at pH 7.2 (R_s = 52 Å for $R_i \leq 33$, R_s = 60 Å for R_i = 65), except that a single peak, with an R_s of 52 Å, is already observed at R_i = 17, indicating a better affinity of the peptide for lipids at acidic pH and for DLPG as compared to DMPG.

The stability of the DLPG complex was tested by incubating preformed complex with DLPG vesicles. At pH 7.2, if DLPG is added to a DLPG–protein complex at R_i = 33 to reach a DLPG/protein ratio of 65 and the new mixture incubated for 10 min, the elution profile shows a single peak eluting at the expected position for a complex with a molar ratio of 65. This indicates that additional lipids are incorporated in the preformed complex. This, together with the occurrence of distinct protein and lipid–protein peaks at lower R_i, suggests a reversible and dynamic character of the association of the fragment with lipids.

At pH 7.2 with the longer chain DPPG, a weaker interaction with the peptide was observed. Although a complex is formed,

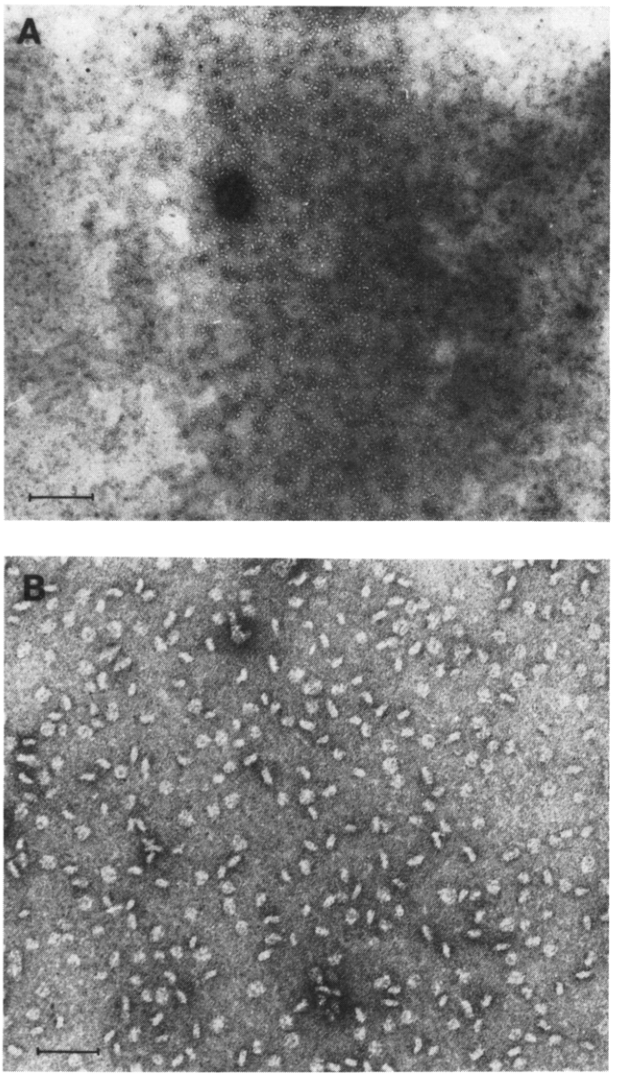

FIGURE 5: Image of the negatively stained DMPG–thermolytic fragment complex: R_i = 25; buffer A, pH 7.2. The complex appears rather homogeneous in size [low magnification (A)]. The particles show two different views, one circular and one rodlike [high magnification (B)]. These two views are consistent with the complex having a disklike shape (60 Å thick, 120 Å in diameter). The bar represents 200 and 40 nm in (A) and (B), respectively.

the peak of free protein never disappears, and above R_i = 33, a small amount of lipid vesicles free of peptide appears (Figure 6A–C). This elution pattern is even more pronounced with DOPG,[2] a lipid with 18 carbon atoms and 1 unsaturated bond

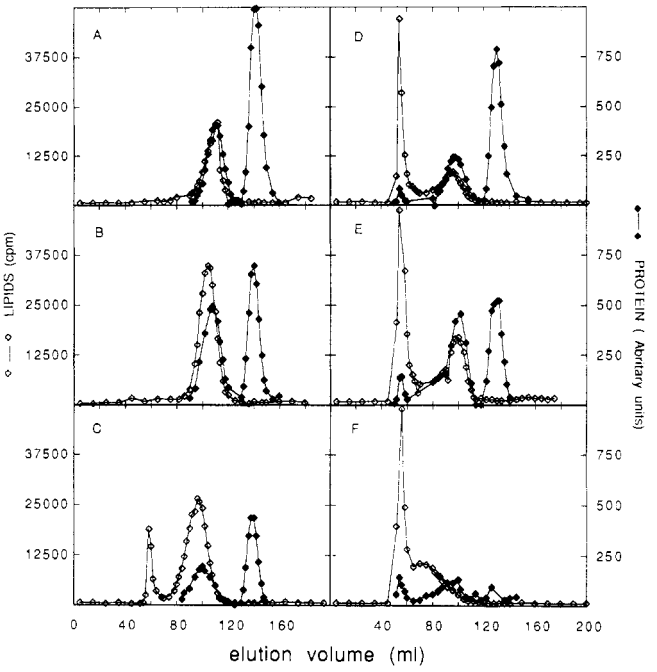

FIGURE 6: Sepharose CL 6B elution profiles of DPPG (A–C) or DOPG (D–F) unilamellar vesicles incubated with colicin A pore-forming fragment at R_i = 17 (A, D), R_i = 33 (B, E), and R_i = 65 (C, F). Same conditions as for Figure 2.

in each of its fatty acid chains (Figure 6D–F). At all ratios tested (from 17 to 100 M/M), the elution profiles show three peaks corresponding to (i) free vesicles, (ii) a complex (R_s = 61 Å), and (iii) free protein. At acidic pH, at the "magic" R_i = 33, both lipids lead to a single lipid–protein complex. However, at a low ratio, protein precipitation occurs as found with DMPG at $R_i < 6$. At ratios above 33, aggregated lipid vesicles are observed.

The influence of the polar headgroup was investigated by incubating the thermolytic fragment at pH 7.2 with DMPC and DMPE vesicles at various lipid/protein ratios and with DMPC/DMPG vesicles at different DMPC/DMPG ratios at R_i = 33. No interaction was found between the thermolytic fragment and the neutral lipids. With DMPC, the column elution profiles were in all cases similar to Figure 2A. Incubation with DMPC/DMPG mixtures showed that, at a DMPC/DMPG ratio of 1/3 M/M and R_i = 33, 50% of the protein is in the complex form. At a DMPC/DMPG ratio of 1/1 M/M, only free vesicles and free protein peaks are observed. This does not exclude peptide binding to the vesicles at these ratios because we are not performing equilibrium gel filtration experiments. Dissociation of weak complexes may thus occur during filtration.

Discussion

The results presented in this study show quite clearly that the pore-forming 20-kDa C-terminal domain of colicin A, monomeric and soluble in water, forms a well-defined oligomeric complex with the negatively charged phospholipid DMPG. The presence of a single peak in the gel filtration profile and a single sedimenting particle in the analytical centrifuge at R_i = 26 demonstrates the high affinity of the protein for this lipid. There is an excellent correlation between gel filtration and analytical centrifugation experiments. The complex dissociates at R_i below 26 and increases in size at R_i values above 33. This complex contains nine peptide monomers and has a disklike shape (60 Å thick, 120 Å in diameter) according to electron microscopy.

The finding of one type of complex containing the C-terminal peptide molecules should not be interpreted as indicating that the ionic channel is formed by a nonamer of this peptide. The size of the complex may reflect the properties of the lipid more than those of the protein. Preliminary cross-linking experiments did not show any evidence of protein oligomers within the complex (data not shown). Colicin A also is monomeric when bound to neutral micelles of phosphatidylcholine analogues (Cavard et al., 1988). However, a rough calculation, using the lipid/protein ratio, the stochiometry of the complex, and the structure of the peptide in solution (Parker et al., 1989), shows that protein/protein contacts may occur within the complex. Assuming that the C-terminal colicin A peptide covers, within the complex, the same area as the surface of the soluble structure proposed to interact with negatively charged lipids (assumed to be a disk 35 Å in diameter; Parker et al., in press), one can calculate that more than 16 lipids are required to form 1 monomolecular layer around 1 monomer. According to electron microscopy, the complex is a disklike particle 60 Å thick (the thickness of a lipid bilayer). Assuming that lipid molecules are arranged in a bilayer structure, more than 32 lipids are required to form a concentric bilayer around the peptide. This rough calculation shows that just the amount of lipids required to form an annulus around each monomer is actually present in the thermolytic fragment–DMPG complex. Moreover, in the DLPG–protein complex at pH 5.0 at an R_i of 17, there are clearly not enough lipids to isolate each monomer. This implies that protein/protein contacts occur within this lipid complex. This is also supported by the continuous increase in size of the complex when the lipid/protein molar ratio is raised from R_i = 6 to R_i = 33 (Table I). The number of peptide molecules remains constant within the complex, but its lipid content increases with the lipid/protein ratio. This result indicates that the protein moiety may play a major role in determining the structure of the complex.

The similarity of the results obtained at neutral and acidic pH contrasts, with previous studies showing that both colicin A and its C-terminal fragment display much stronger lipid affinity in lipid monolayer and vesicles at acidic pH (Pattus et al., 1983; Frenette et al., submitted for publication). The origin of these discrepancies lies in the difference of the ionic strength of the buffer used in these studies. At pH 7, 0.1 M NaCl is sufficient to inhibit complex formation while at pH 5.0 it has no effect (data not shown). Ionic strength has a dual effect on the binding and insertion of the peptide to membranes: a decrease in the ionic interactions between the protein and lipids and a stabilization of the soluble structure of the peptide, increasing the energy costs of unfolding which precedes membrane insertion. This dual effect of ionic strength may amplify the effect of pH on peptide–lipid affinity.

The influence of the nature of the phospholipid headgroup on the protein/lipid interaction demonstrates that, as with colicin A, the C-terminal domain needs negatively charged headgroups to bind and insert into the membrane. They do not contradict the previous study showing that colicin A binds to micelles of neutral lecithin analogues (Cavard et al., 1988). Negative charges on the membrane surface may be required only for binding and insertion into well-packed bilayers and not in lipid micelles. These results support the model of interaction proposed by Parker et al. (1989), based on the crystal structure of the peptide. The peptide in solution contains a hydrophobic hairpin initially buried inside the protein. It is thought that binding to the negatively charged lipid interface through the positively charged face of the structure orients

[2] DOPG was chosen instead of its saturated homologue because of its lower phase transition temperature.

the hydrophobic hairpin perpendicular to the plane of the membrane. This hairpin would then provide the driving force to insert the protein into the lipid bilayer and to stabilize the lipid–protein complex. The remaining amphipatic helices would remain at the surface on one side of the bilayer. This model may explain why this peptide interacts better with short-chain lipids. The hydrophobic hairpin is only 16–17 residues long and thus shorter than a bilayer formed by phospholipid molecules such as DOPG or DPPG. The short-chain DLPG and DMPG would accommodate better the length of the hairpin.

Similar discoidal lipid–peptide or detergent–lipid complexes have been observed with bile salt–lipid complexes (Small, 1967; Mazer et al., 1980) and surface-active peptides such as apolipoproteins from human serum, mellitin, calcitonin, and glucagon and leader peptides from imported mitochondrial proteins [see Segrest (1977), Dasseux et al. (1984), Dufourcq et al. (1986), and Epand et al. (1983, 1986) and references cited therein]. It was proposed that these discoidal micelles consist of a lipid bilayer stabilized on its edges by a ring of bile salt molecules or amphipathic helices. By analogy, the amphipathic helices of the pore-forming domain of colicin A may stabilize similarly discoidal lipid–protein complexes. However, analysis of the distribution of positively charged residues and the presence of the hydrophobic hairpin in the thermolytic fragment structure (Parker et al., 1989) suggest a different mechanism of initial interaction with the membrane. These positively charged residues belong to the extremities of different amphipatic helices and form a ring around the hairpin. In this initial interaction, the amphipathic helices would not lie parallel to the plane of the membrane. In addition, as suggested for the first time by Engelman and Steitz (1981), the hydrophobic hairpin may provide most of the energy for membrane insertion of the colicin fragment.

The results of the present study do not indicate whether the lipid molecules are arranged as a bilayer and whether the "bicycle tyre" model from Segrest (1977) applies to the thermolytic fragment–lipid complex. We are currently investigating these points by applying spectroscopic and biochemical methods to the study of this complex.

ACKNOWLEDGMENTS

We thank Nathalie Didat and Marie-Pierre Reck for excellent technical assistance and Christine Barber for assistance in preparing the manuscript. We acknowledge J. Lakey, H.-U. Wilmsen, M. Parker, C. Lazdunski, and F. Heitz for many fruitful discussions and critical readings of the manuscript.

REFERENCES

Adrian, M., Dubochet, J., Lepault, J., & McDowall, A. W. (1984) *Nature 308*, 32–36.

Babul, J., & Stellwagen, E. (1969) *Anal. Biochem. 28*, 216–221.

Bull, H. B., & Breese, K. (1974) *Arch. Biochem. Biophys. 161*, 665–670.

Casassa, E. F., & Eisenberg, H. (1964) *Adv. Protein Chem. 19*, 287–395.

Cavard, D., & Lazdunski, C. (1979) *Eur. J. Biochem. 96*, 517–524.

Cavard, D., Sauve, P., Heitz, F., Pattus, F., Martinez, C., Dijkman, R., & Lazdunski, C. (1988) *Eur. J. Biochem. 172*, 501–512.

Cohn, E. J., & Edsall, J. T. (1943) in *Proteins, Amino Acids and Peptides*, pp 157–161, 370–375, Reinhold, New York.

Collarini, M., Amblard, G., Lazdunski, C., & Pattus, F. (1987) *Eur. Biophys. J. 14*, 147–153.

Dasseux, J.-L., Faucon, J.-F., Lafleur, M., Pezolet, M., & Dufourcq, J. (1984) *Biochim. Biophys. Acta 775*, 37–50.

Dufourcq, J., Faucon, J.-F., Fourche, G., Dasseux, J.-L., Le Maire, M., & Gulik-Krzywicki, T. (1986) *Biochim. Biophys. Acta 859*, 33–48.

Engelman, D. M., & Steitz, T. A. (1981) *Cell 23*, 411–422.

Epand, R. M., Epand, R. F., Orlowski, R. C., Sclueter, R. J., Boni, L. T., & Hui, S. W. (1983) *Biochemistry 22*, 5074–5084.

Epand, R. M., Hui, S. W., Argan, C., Gillepsie, L. L., & Shore, G. C. (1986) *J. Biol. Chem. 261*, 1017–1020.

Homo, J.-C., Booy, F., Labouesse, P., Lepault, J., & Dubochet, J. (1984) *J. Microsc. (Oxford) 136*, 337–340.

Hui, S. W., Epand, R. M., Dell, K. R., Epand, R. F., & Orlowski, R. C. (1984) *Biochim. Biophys. Acta 772*, 264–272.

Lazdunski, C., Baty, D., Geli, V., Cavard, D., Morlon, J., Lloubes, R., Howard, P., Knibiehler, M., Chartier, M., Varenne, S., Frenette, M., Dasseux, J.-L., & Pattus, F. (1988) *Biochim. Biophys. Acta 947*, 445–464.

Le Maire, M., Ghazi, A., Moller, J. V., & Aggerbeck, L. P. (1987) *Biochem. J. 243*, 399–404.

Martinez, M. C., Lazdunski, C., & Pattus, F. (1983) *EMBO J. 2*, 1501–1507.

Parker, M. W., Pattus, F., Tucker, A. D., & Tsernoglou, D. (1989) *Nature 337*, 93–96.

Pattus, F., Martinez, M. C., Dargent, B., Cavard, D., Verger, R., & Lazdunzski, C. (1983) *Biochemistry 22*, 5698–5703.

Reynolds, J. A., & Tanford, C. (1976) *Proc. Natl. Acad. Sci. U.S.A. 73*, 4467–4470.

Schein, S. J., Kagan, B. L., & Finkelstein, A. (1978) *Nature (London) 276*, 159–163.

Segrest, J. P. (1977) *Chem. Phys. Lipids 18*, 7–22.

Tokuda, H., & Konisky, J. (1979) *Proc. Natl. Acad. Sci. U.S.A. 76*, 6167–6171.

Tucker, A. D., Pattus, F., & Tsernoglou, D. (1986) *J. Mol. Biol. 190*, 133–134.

Valentine, R. C., Shapiro, B. M., & Stadtman, E. R. (1968) *Biochemistry 7*, 2143–2152.

Yphantis, D. A. (1964) *Biochemistry 3*, 297–317.